Accepted Manuscript

Analysis of the red ochre of the El Mirón burial (Ramales de la Victoria, Cantabria, Spain)

Romualdo Seva Román, Cristina Biete Bañón, Mª Dolores Landete Ruiz

PII: S0305-4403(15)00126-0

DOI: 10.1016/j.jas.2015.03.033

Reference: YJASC 4403

To appear in: *Journal of Archaeological Science*

Received Date: 30 December 2014

Revised Date: 26 March 2015

Accepted Date: 27 March 2015

Please cite this article as: Román, R.S., Bañón, C.B., Landete Ruiz, M.D., Analysis of the red ochre of the El Mirón burial (Ramales de la Victoria, Cantabria, Spain), *Journal of Archaeological Science* (2015), doi: 10.1016/j.jas.2015.03.033.

ANALYSIS OF THE RED OCHRE OF THE EL MIRÓN BURIAL (Ramales de la Victoria, Cantabria, Spain)

Romualdo Seva Román[a] , Cristina Biete Bañón[b], Mª Dolores Landete Ruiz[b].

[a]Archaeometry Unit, Research Technical Services; Dept. of Ecology. University of Alicante. Ctra. San Vicente s/n. E-03690. Alicante. Spain.

[b] Archaeometry Unit, Research Technical Services. University of Alicante. Ctra. San Vicente s/n. E-03690. Alicante. Spain.

*Corresponding author. Tel: +34 610488927.

E-mail addresses: romualdo.seva@ua.es, (Romualdo Seva Román), cristina.biete@ua.es, (Cristina Biete Bañón), md.landete@ua.es, (Mª Dolores Landete Ruiz).

ABSTRACT

This article analyzes the ochre associated with the human burial of Magdalenian age in El Mirón Cave that, with its unique features (deep red color, brightness and particle size distribution), is clearly differentiated from ochres in other strata of the site.

The most common techniques in archaeological pigment characterization studies were used: binocular microscope inspection, thin sections, granulometry, X-ray diffraction (XRD), scanning electron microscopy (SEM-EDX), X-ray fluorescence (XRF), Raman spectroscopy and inductively coupled plasma mass spectrometry (ICP-MS).

The results obtained permit the characterization of special ochre in burial layer (hematite with idiomorphic crystallinity). Its origin is completely different from the samples from outcrops inside El Mirón Cave or obtained by prospecting in Carranza Valley. This type of hematite has been identified on the coast, in Santoña, about 26 km from the burial. Given its uniqueness, can be associated with some kind of spiritual rite of the time whose backgrounds are in the Middle Palaeolithic and continuing for the rest of Prehistory.

Key words: Magdalenian burial, El Mirón Cave, ochre, hematite, thin section, XRD, SEM-EDX, XRF, Raman spectroscopy, ICP-MS, idiomorphic hematite.

1. INTRODUCTION

The study of prehistoric ochre has mainly been focused on the analysis of raw materials and their uses (Eiselt et al., 2011; Marshall et al., 2005; Mooney et al., 2003; Popelka-Filcoff et al., 2007, 2008) (including for cave paintings [Hernanz et al., 2010; Iriarte et al., 2009], both by modern humans and by earlier species, including European Neandertals (Zilhão, 2001).

Numerous methods have been successfully tested to determine the nature and the provenance of the raw materials, such as scanning electron microscopy coupled with energy dispersive X-ray spectrometry (SEM-EDX), proton induced X-ray emission (PIXE), X-ray diffraction (XRD), FTIR and Raman spectrometry, X-Ray fluorescence (XRF), inductively coupled plasma mass spectrometry (ICP-MS), or instrumental neutron activation analysis (INAA) (see Beck et al. 2011; Bikiaris et al., 2000; David et al., 1993; d'Errico et al.; 2010; Eiselt et al., 2011;

Jercher et al., 1998; Macdonald et al., 2013; Popelka-Filcoff et al., 2007, 2008; Scadding et al., 2015; Smith and Fankhauser, 2009).

The use of ochre in rituals is well documented in South Africa 75 kya (Dayet et al., 2013; Henshilwood et al., 2001, 2009; Rifkin, 2012), Mediterranean Levant and Europe since 60-40 kya, during the late Middle and early Upper Paleolithic (d'Errico et al., 1998, 2010; Hovers et al., 2003; Roebroeks et al., 2012; Zilhão et al., 2010), with a significant increase during the Gravettian (ca. 30-20 uncal. kya), particularly in burials, from Portugal and Wales to Russia.

Among the many strata excavated in the extensively studied El Mirón Cave (e.g., González-Morales and Straus, 2000, 2009; Straus et al., 2002; Straus and González-Morales, 2003, 2012a, 2012b), is Level 504, which contained the human burial preliminarily described by Straus et al. (2011) and studied in detail in this special issue of *JAS*. This level is composed essentially of hematite and iron oxides mixed with silt, limestone gravel, organic matter such as charcoal, lithic artifacts and bones. Its bright, dark red color distinguishes it from all other strata in the cave.

The sediments used to cover the burial were mixed with hematite specially extracted from particular outcrops, suggesting deep ritual connotations. It is noteworthy that (although degraded) the color of the pigment staining the eastern face of the large engraved block adjacent to the burial matches that of the ochre in the sediments of the grave. This pigment has not been analyzed in this study to understand that could be put in relation to the rest of the paintings from The Mirón cave in further researches.

This article concludes that special ochre was used for covering the body, defined by its unique features and suggests its possible origin, differentiating it, from other ochres found in Magdalenian levels of El Mirón, where they seem to have had other (non-funerary) uses.

2. MATERIAL AND METHODS

The materials analyzed are 24 ochres collected in the stratigraphy of the various Magdalenian occupations reservoir and 4 samples of stratigraphic units 503, 504, 505 and 506 of X7 square (Table 1; Figures 1-6).

Other ochres from known ferrous outcrops that we sampled in the Upper and Middle Carranza River valley (provinces of Vizcaya and Cantabria, approximately 10-20 km from El Mirón) were also analyzed.

Samples 1-12 are small pieces of ochre selected from sediments during excavation, in different squares: J2, J4 (level 17); T9 (level 116), U9 (level 119 and 119.2), U10 (level 119 and 119.2), V10 (level 120) and X7 (level 501 and 504) -Figures 1 and 2. All ochres chronologically fit between the Initial and Lower Magdalenian period. The total sample weight is about 1 gram.

Some samples are from the same level and square: samples 6A, 6B and 6C (U10 square - level 119), and 7A and 7B (U9 square - level 119.2).

Samples 1M to 9M belong to the V9 square (Initial and Lower Magdalenian). They were selected by their nature and different colors as shown in Figure 6 (for example, 2M and 3M samples were selected for their metallic luster. The total sample weight is about 1 gram.

Samples 11 and 12 correspond to the bedding cover burial, 504 (clearly differentiated from level 503 and 505, as seen in Figure 5). All the level 504 showed very small bright fragments, which later were identified like hematite. Also appeared ochres fragment visually reddish and brown – violet (Image 10, 11 and 12, Figure 6).

Sediment samples (about 100 grams) were also selected to analyze the burial stratigraphic context.

The ochre samples were first dried at 100 °C in an oven overnight, to remove moisture. These samples were used to thin sections, binocular microscope inspection and microscopy studies.

The dried samples were ground into powder using an agate mortar and pestle, and powder samples were analyzed by inductively coupled mass spectrometry, Raman spectroscopy, X-ray diffraction and X-ray fluorescence spectrometry.

We employed the following analytical methods and instrumentation:

A Nikon SMZ 645 binocular microscope (with 8-50 magnification), was used to observe the morphological structure of the ochres.

Mineralogical analysis of ochre in thin sections was performed using a Nikon OPTIPHOT 2 – POL polarized light microscope. Images were captured by a Color View 12 camera with a Soft Imaging System.

Scanning electron microscopy (SEM) was applied in order to obtain the elemental composition of the samples in terms of percentages of the main chemical elements by means of an energy-dispersive X-ray microanalysis probe (EDX). We used an Hitachi S-3000N device, equipped with a secondary electron detector (photomultiplier type e 3.5 nm resolution), a semiconductor backscattered electron detector (5 nm resolution), as well as an X-ray detector that was able to detect elements from carbon to uranium. We also studied the structural morphology of the ochre. The scanning microscope is able to work in variable pressure mode for observation of nonconductive specimens without coating with any conductive material. Different samples were chosen from level 504: reddish ochre, fragments rich in hematite (small and bright), and sediment. Also a sample from Carranza River prospection was analyzed.

The composition of the samples was confirmed with X-ray fluorescence spectrometry (XRF), using a PW2400 Philips MagiX PRO instrument with SuperQ-IQ+ software.

Mineral composition of the samples was measured on a Bruker D8 Advance X-ray Diffractometer, with CuKα radiation (40 kV, 40 mA). Each sample was scanned over the 2-theta range 4-85º with a step size of 0.05º and a count time of 3 s per step. The obtained X-ray diffractograms were interpreted using the DIFFRAC plus Basic, Evaluation Release 2009 software.

Raman spectra were recorded using a LabRAM Jobin-Yvon HORIBA Raman dispersive spectrometer, with a laser emitting at 633 nm. The power radiation measured under the Nikon x50 microscope objective was about 0.4 mW. The spectra were recorded as a sum of two 100 second scans. The calibration of the spectrometer was done with a Si standard (main band: 520,5 cm^{-1}).

Trace elements were analysed by inductively coupled mass spectrometry on a THERMO ELEMENTAL VG PQ-ExCell equipment. Samples were digested at 220° C with a mixture of nitric and hydrochloric acids in a microwave oven system (Milestone Start D). 250 mg of sample was placed in a PTFE reactor with 4mL HNO3 and 4mL HCl. The heating procedure consists of a first step of 10 min to reach 220ºC and a second step of 20 min at 220ºC. After cooling, sample digests were transferred into a 25mL flask and brought to volume with MilliQ water. Quantities in ppm (mg/Kg) of the different atomic elements present in the samples were determined. Mass sample and dilution were considered. Three replicates were run for each sample.

3. RESULTS AND DISCUSSION.

The granulometry of Level 504 shows small-size gravels with a high percentage of fine fraction (78% <2mm) including a clayey ochre (powder) and larger particles with bright fragments observed through the binocular microscope (hexagonal-system crystal hematite), with subconchoidal fractures.

The thin-section analysis shows clear differences between natural ochre samples from the Upper and Middle Carranza outcrops and hematite from the burial (Figure 7).

The specimens from the Upper and Middle Carranza Valley are defined by crystal calcite, goethite and quartz, plus ferric clays, while the hematite from the burial is clearly crystalline.

Its different genesis can also be seen in the association of large quartz - calcite crystals with amorphous iron from the samples we collected by prospecting in the region around the site; conversely, the Level 504 ochre has the crystal structure defined above.

The results obtained by X-ray diffraction (XRD), show a clear sedimentological differentiation of Level 504 from the occupation levels above and below it (503, 505 and 506), where hematite or other iron oxides do not appear (Figure 8). The composition of these horizons is mainly quartz, calcite, and to a lesser extent, anorthite and microcline, and in some cases

dolomite. (Note that calcite-dolomite association occurs in limestone formations of this area, as can be seen in the geological maps [IGME, 1974a,b; 1978, 1982; Vera, 2004]). The presence of apatite in virtually all levels must be related to the abundant osseous remains of the site.

By contrast, the iron oxides of 504, contains a high percentage of crystalline hematite. This mineral could be distinguished in sediment by color and brightness, and the diffractogram peak 2.69 - 2.70 confirmed it (Figure 8e). These results show that the ochre burial fill was clearly intentional and presumably related to ritual practices of the time (Dayet et al., 2013; d'Errico et al., 1998, 2010; Henshilwood et al., 2001, 2009; Hovers et al., 2003; Rifkin, 2012; Roebroeks et al., 2012; Zilhão et al., 2010).

Even more enlightening is the morphological study by scanning electron microscopy, confirming the results obtained with the binocular microscope and thin-section analysis. The massive iron structure is clearly distinguishable in the samples from the Upper and Middle Carranza Valley, compared to the hematite used in the burial fill (Figure 9, Table 2).

Data obtained by SEM-EDX were collected after an exploratory scanning. As can be seen in Table 2 and Figure 9, there are cristalline hematite. Carbon percentage should mainly be attributed to the tape used for fixing the sample in the sample holder and any trace organic residue.

The hematite level 504 is clearly defined by its leafy habit and crystallinity in the hexagonal system. The sediment shows high iron oxide content, mainly hematite (Figure 9c). The sample of Carranza Valley, although it is very rich in iron oxides (hematite peak 2.69 to 2.70 XRD), has a completely different morphology.

The analysis of samples by XRF (Table 3) shows no correlation between iron with other elements.

Knowing the characteristics of the metallographic areas of the basins of Asón and Carranza Rivers, associations of iron with lead, zinc and copper can occur (IGME, 1974b).

Raman spectroscopy was employed to characterize some ochre samples from the Cave (2, 12 – hematite Level 504 and 1M), and a sample from the prospection survey (2P).

Hematite belongs to the D^6_{3d} crystal space group and seven phonon lines are expected in the Raman spectrum, namely two A_{1g} modes (225 and 498 cm^{-1}) and five E_g modes (247, 293, 299, 412 and 613 cm^{-1}) (de Faria et al., 1997). A broad medium band may be moreover recorded near 1320 cm^{-1}, which is assigned to a 2^{nd} harmonic vibration (Zoppi et al., 2005).

All the samples display characteristic hematite mineral bands, with differences in the relative intensities of the bands.

The spectrum of a perfect hematite crystal should not present any signal near 660 cm^{-1}, but this band does appear in many spectra, depending on the type of material studied. Recent studies assign the origin of this band to impurities, and therefore, it appears in the less crystalline samples (Bikiaris et al., 1999; Zoppi et al., 2005).

The analyzed samples present a fairly strong band at 661 cm^{-1}, except for the sample from Level 504, where this band is very small, which means that this ochre is much more crystalline compared to the others. This differentiation would be also supported by the definition of the peak of hematite obtained by XRD.

The area of the main peaks (*a, b, c, d* and *e*) of the selected spectra (one for each sample) were calculated. Peak *b* remained stable; its peak intensity was therefore taken as a reference peak measurement. Table 4 shows peak position (cm^{-1}), and values of ratios of peak areas for the studied ochres. Peak *e* is a double peak, and the total area was calculated.

The area ratio distinguishes 504 ochre level from the rest. These data confirm that the ochre used for the burial is of a different nature than the rest of ochre materials in the cave, as well as from the Carranza Valley prospection samples, highlighting the special properties of the type of hematite used for covering the burial.

The analysis of ochre trace elements obtained by ICP-MS is crucial to establish their origin (Iriarte et al., 2009; Smith and Fankhauser, 2009), as well as to provide information on the use of different sources during the Initial, Lower and Middle Magdalenian periods in El Mirón Cave.

These data were statistically compared by analyzing the principal components (Todd and Leonard, 2010) with SPSS Statistics 21.

The statistical results define different groups of ochre samples from Initial and Lower Magdalenian levels, those covering the burial, and those from our prospection in the Carranza Valley (Figure 11).

In view of the results, the following groups can be established:

- Group 1. Samples 3M, 4M, 6M, 7M and 8M of El Mirón, associated with Initial and Lower Magdalenian levels.

- Group 2. Ochre samples from the upper and middle Carranza Valley (1P, 2P, 4P, 5P, 6P and 7P).

- Group 3. Iron oxide from the Carranza headwaters area (3P).

- Group 4. Ochre samples selected from the Level 504 burial fill (EU.504-504 A and B).

- Group 5. Ochre 5M from El Mirón Initial & Lower Magdalenian occupation levels.

- Group 6. Very different from the rest of the ochres, but also from the Lower & Middle Magdalenian occupation levels of El Mirón Cave (9M).

These results differentiate the burial ochre from all the other samples, although we have not been able to determine the source area thereof.

4. CONCLUSIONS.

During the Initial, Lower and Middle Magdalenian periods, the inhabitants of El Mirón Cave used a special ochre to cover the burial, at this time known level 504.

The analysis of ochre found in this level, by several analytical methods, and their comparison with others samples in the same Cave and nearby prospections, has confirmed their singularity and special features.

This ochre can be distinguished visually from the rest of those found in the Magdalenian occupation levels of the site or prospections in Carranza Valley. SEM-EDX, thin section, XRD and Raman analysis have confirmed the high crystallinity and they have allowed the study of the morphology and mineralogy. It is a hematite with leafy habit and hexagonal crystals, very different from the rest of iron oxides and hematite.

Its origin, although impossible to determine by analytical comparison, is completely different from that of the samples obtained by prospecting. This leaves open the possibility to locate it in as yet unknown outcrops with hematite crystalline forms.

After reviewing the literature on Cantabrian mining, the closest massive hematite outcrops exist in Santoña (Monte Muciero, -now barely detectable due to urban development and reforested areas-), about 26 km from the cave (Figure 12). This might be the source area of this iron ore.

To conclude, we can say the inhabitants of El Mirón carefully chose this bright crystalline hematite and combined with other iron oxides finely distributed over the cadaver. They walked tens of kilometers to take it inside the cave and then give the ritual burial that Lady of Myron deserved and preserved she to ours days. We do not really know the social importance of this personage; maybe someday we can know something more.

Acknowledgments

The project was financed by the Spanish Ministry of Science and Technology (HAR2010-22115-C02-02). We also thank José Bautista, Andrés Amorós, Alejandro Jareño, Clemente Santana, Jerónimo Juan and María Teresa Ferrándiz, staff from several Units of the Research Technical Services and from the Office of the Vice President for Research at the University of Alicante. Finally we also acknowledge the support of Eduard and Anna Seva in this work and Mikel Lopez

Horgue for invaluable assistance with the prospection. The manuscript was edited by L.G. Straus.

REFERENCES.

Beck, L., Lebon, M., Pichon, L., Menu, M., Chiotti, L., Nespoulet, R., Paillet, P., 2011. PIXE characterisation of prehistoric pigments from Abri Pataud (Dordogne, France). X-Ray Spectrometry 40 (3), 219-223.

Bikiaris, D., Daniilia, S., Sotiropoulou, S., Katsimbiri, O., Pavlidou, E., Moutsatsou, A. P., Chryssoulakis, Y., 1999. Ochre-differentiation through micro-Raman and micro-FTIR spectroscopies: Application on wall paintings at Meteora and Mount Athos, Greece. Spectrochimica Acta - Part A: Molecular and Biomolecular Spectroscopy 56 (1), 3-18.

David, B., Clayton, E., Watchman, A. L., 1993. Initial Results of PIXE Analysis on Northern Australian Ochres. Australian Archaeology, 36, 56-57.

Dayet, L., Texier, P. J., Daniel, F., Porraz, G., 2013. Ochre resources from the Middle Stone Age sequence of Diepkloof Rock Shelter, Western Cape, South Africa. Journal of Archaeological Science 40 (9), 3492-3505.

De Faria, D.L.A., Silva, S.V., de Oliveira, M.T., 1997. Microspectroscopy of Some Iron Oxides Raman and Oxyhydroxides. Journal of Raman Spectroscopy 28, 873-878.

D'Errico, F., Zilhão, J., Julien, M., Baffier, D., Pelegrin, J., 1998. Neanderthal Acculturation in Western Europe?. A Critical Review of the Evidence and Its Interpretation. Current Anthropology 39, S1-S44.

D'Errico, F., Salomon, H., Vignaud, C., Stringer, C., 2010. Pigments from the Middle Palaeolithic levels of Es-Skhul (Mount Carmel, Israel). Journal of Archaeological Science 37, 3099-3110.

Eiselt, B.S., Popelka-Filcoff, R.S, Darling, J.A., Glascock, M.D., 2011: Hematite sources and archaeological ochres from Hohokam and O'odham sites in central Arizona: an experiment in type identification and characterization. Journal of Archaeological Science 38, 3019-3028.

González-Morales, M.R., Straus, L.G., 2000. La cueva del Mirón (Ramales de la Victoria, Cantabria): Excavaciones 1996-1999, Trabajos de Prehistoria 57, 121-133.

González-Morales, M. R., Straus, L.G., 2009. Extraordinary Early Magdalenian finds from El Mirón Cave, Cantabria (Spain). Antiquity 83, 267–281.

Henshilwood, C. S., Sealy, J. C., Yates, R., Cruz-Uribe, K., Goldberg, P., Grine, F. E., Klein, R. G., Poggenpoel, C., Van Niekerk, K., Watts, I., 2001. Blombos Cave, southern Cape, South Africa: Preliminary report on the 1992-1999 excavations of the Middle Stone Age levels. Journal of Archaeological Science 28 (4), 421-448.

Henshilwood, C. S., d'Errico, F., Watts, I., 2009. Engraved ochres from the Middle Stone Age levels at Blombos Cave, South Africa. Journal of Human Evolution 57, 27-47.

Hernanz, A., Ruiz-López, J.F., Gavira-Vallejo, J.M., Martín, S., Gavrilenko, E., 2010. Raman microscopy of prehistoric rock paintings from the Hoz de Vicente, Minglanilla, Cuenca, Spain. Journal of Raman Spectroscopy 41, 1394–1399.

Hovers, E., Shimon, I., Bar-Yosef, O., Vandermeersch, B., 2003. An early case of color symbolism: ochre use by modern humans in Qafzeh Cave. Current Anthropology 44 (4), 491-522.

Kiehn, A.V., Brook, G.A., Glascock, M.D., Dake, J.Z., Robbins, L.H., Campbell, A.C., Murphy, M.L., 2007. Fingerprinting specular hematite from mines in Botswana, southern Africa. In: Glascock, M.D., Speakman, R.J., Popelka-Filcoff, R.S. (Eds.), Archaeological Chemistry. American Chemical Society, Washington, pp. 460-479.

IGME, 1974: Mapa Metalogenético de España 1:200.000. Hoja correspondiente a Bermeo. Servicio de Publicaciones del Ministerio de Industria. Madrid.

IGME, 1974: Mapa Metalogenético de España 1:200.000. Hoja correspondiente a Bilbao. Servicio de Publicaciones del Ministerio de Industria. Madrid.

IGME, 1978: Mapa geológico de España 1:50.000. Hoja correspondiente a Valmaseda. Servicio de Publicaciones del Ministerio de Industria. Madrid.

IGME, 1982: Mapa geológico de España 1:50.000. Hoja correspondiente a Castro Urdiales. Servicio de Publicaciones del Ministerio de Industria. Madrid.

Iriarte, E., Foyo, A., Sánchez, M.A., Tomillo, C., Setién, J., 2009. The origin and geochemical characterization of red ochres from the Tito Bustillo and Monte Castillo Caves (northern Spain). Archaeometry 51, 231-251.

Jercher, M., Pring, A., Jones, P. G., Raven, M. D., Rietveld, 1998. X-Ray Diffraction and X-Ray Fluorescence analysis of Australian Aboriginal Ochres. Archaeometry 40 (2), 383-401.

Macdonald, B. L., Hancock, R. G. V., Cannon, A., McNeill, F., Reimer, R., Pidruczny, A., 2013. Elemental Analysis of Ochre Outcrops in Southern British Columbia, Canada. Archaeometry 55(6), 1020-1033.

Marshall, L.R., Williams, J.R., Almond, M.J., Atkinson, S.D.M., Cook, S.R., Matthews, W., Mortimore, J.L., 2005. Analysis of ochres from Clearwell Caves: the role of particle size in determining color. Spectrochimica Acta Part A 61, 233–241.

Mooney S.D., Geiss C., Smith, M.A., 2003. The use of mineral magnetic parameters to characterize archaeological ochers. Journal of Archaeological Science 30, 511-523.

Popelka-Filcoff, R.S., Robertson, J.D., Glascock, M.D., Descantes, Ch. 2007. Trace element characterization of ochre from geological sources. Journal of Radioanalytical and Nuclear Chemistry 272, 17–27.

338 Popelka-Filcoff, R.S., Miksa, E.J., Robertson, J.D., Glascock, M.D. & Wallace, H., 2008. Elemental
339 analysis and characterization of ochre sources from southern Arizona. Journal of
340 Archaeological Science 35, 752–762.

341 Rifkin, R.F. 2012. Processing ochre in the Middle Stone Age: Testing the inference of
342 prehistoric behaviours from actualistically derived experimental data. Journal of
343 Anthropological Archaeology 31 174–195.

344 Roebroeks, W., Sier, M.J., Nielsen, T.K., De Loecker, D., Parés, J.M., Arps, C.E.S., Mücher, H.J.,
345 2012. Use of red ochre by early Neandertals. Proceedings of the National Academy of Sciences
346 109, 1889-1894.

347 Roldan-Garcia, C., Vanhaeren, M., Villaverde, V., Wood, R., & Zapata, J., 2010. Symbolic use of
348 marine shells and mineral pigments by Iberian Neandertals. Proceedings of the National
349 Academy of Sciences of the United States of America 107, 1023-1028.

350 Scadding, R., Winton, V., Brown, V., 2015. An LA-ICP-MS trace element classification of ochres
351 in the Weld Range environ, Mid West region, Western Australia. Journal of Archaeological
352 Science 54, 300-312.

353 Smith, M. and Fankhauser, B., 2009. Geochemistry and identification of Australian red ochre
354 deposits. Palaeoworks Technical Papers 9. National Museum of Australia and Centre for
355 Archaeological Research. Australian National University, Australia.

356 Straus, L.G., González-Morales, M.R., Fano-Martínez, M.A., García-Gelabert, M.P., 2002. Last
357 Glacial Human Settlement in Eastern Cantabria (Northern Spain). Journal of Archaeological
358 Science 29, 1403–1414.

359 Straus, L.G., González Morales, M.R., 2003. Early-mid Magdalenian Excavations in El Mirón
360 Cave Ramales, Cantabria, Spain: Report on the VII Campaign 2002. Eurasian Prehistory 1 (2),
361 117-137.

362 Straus, L.G., González-Morales, M.R., Carretero, J. M., 2011. Lower Magdalenian secondary
363 human burial in El Mirón Cave, Cantabria, Spain. Antiquity 85, 1151–1164.

364 Straus, L.G., González-Morales, M. R., (Eds.), 2012a. El Mirón Cave, Cantabrian, Spain: The Site
365 and Its Holocene Archaeological Record. University of New Mexico Press, Alburquerque.

366 Straus, L.G., González-Morales, M. R., 2012b. The Magdalenian settlement of the Cantabrian
367 region (Northern Spain): The view from El Mirón Cave. Quaternary International 272-373, 111-
368 124.

369 Todd, L., Leonard, R.D., 2010. Quantitative analysis in Archeology. Wiley-Blackwell, Oxford, UK.

370 Vera, J.A. (Ed.), 2004. Geología de España. SGE-IGME, Madrid.

371 Zilhão, J. 2001. Neandertal/modern human interaction in Europe. In: Thacker, P., Hays, M.
372 (Eds.), Questioning the Answers: Resolving Fundamental Problems of the Early Upper
373 Paleolithic. British Archaeological Reports International Series 1005, Oxford, pp. 13-19.

374 Zilhão, J., Angelucci, D., Badal-Garcia, E., d'Errico, F., Floreal D., Dayet, L., Douka, K., Higham,
375 T., Martinez-Sanchez, M.J., Montes-Bernardez, R., Murcia-Mascaros, S., Perez-Sirvent, C.,
376 Roldan-Garcia, C., Vanhaeren, M., Villaverde, V., Wood, R., Zapata, J. 2010. Symbolic use of
377 marine shells and mineral pigments by Iberian Neandertals. In: Proceedings of the National
378 Academy of Sciences of the United States of America, Vol. 107, No. 3, p. 1023-1028.

379 Zoppi, A., Lofrumento, C., Castellucci, E.M., Migliorini, M.G., 2005. The Raman spectrum of
380 hematite: possible indicator for a compositional or firing distinction among *Terra Sigillata*
381 wares. Annali di Chimica 95.

Table 1. Description of analyzed samples.

	Sample	Level	Square
Ochres	1	17	J4
	2	17	J2
	3	116	T9
	4	119	U9
	5	119	U9
	6A 6B 6C	119	U10
	7A 7B	119.2	U9
	8	119.2	U10
	9	120	V10
	10	501	X7
	11 (504A)	504	X7
	12 (504B)	504	X7
	1M	Lower and Middle Magdalenian	
	2M		
	3M		
	4M		
	5M		
	6M		
	7M		
	8M		
	9M		
	1P	Prospection of the headwaters Carranza River	
	2P		
	3P		
	4P		
	5P		
	6P		
	7P		
Sediments	503 sed	503	X7
	504 sed	504	X7
	505 sed	505	X7
	506 sed	506	X7

Table 2. Elemental composition obtained by SEM-EDX (%).

Sample	Fe	Si	Al	K	Mg	C	O	Mn
Ochre EU 504	55,39	0,92	0,67			7,71	35,31	
Hematite EU 504	42,41	0,15	0,72			12,99	43,72	
Hematite EU 504 – Area without impurities	60,51					14,7	24,79	
Sediment EU 504	33,75	5,48	3,28	0,55		7,52	20,04	
2P	43,81	0,61			0,98	11,85	42,03	0,73

Table 3. Normalized elemental composition (%), obtained by X-ray fluorescence (XRF).

Sample	Fe	Al	Ca	Si	K	Ti	Zr	P	Mn	Zn	Mg	Cu	Pb	As	Ba	S	Sr	Na	Cr	Rb
1	98,53	0,88	0,01		0,22				0,24				0,12							
2	89,53	8,91	0,01		1,31	0,18													0,06	
3	17,92	27,26	46,87		6,31	1,53	0,09	0,02												
4	0,66	13,45	61,40		3,38		0,02	20,52		0,12		0,29				0,08	0,08			
5	77,15	5,99	0,01	14,46	1,44	0,15		0,01	0,17		0,62									
6A	83,36		0,01		0,61			0,01	0,25						15,12	0,55	0,09			
6B	24,62	15,43	0,02	49,60	8,84	0,85	0,05		0,38	0,07						0,09	0,02			0,03
6C	20,27	16,09	0,02	51,51	8,57	0,73	0,04		0,26		2,32					0,17	0,02			
7A	86,27	1,14			0,54				0,12	0,05								11,87		
7B	86,16	1,16	0,01	6,63	4,87			0,01		0,12						1,04				
8	92,65	3,29	0,01		1,03	0,21		0,01	0,82	0,66	0,64	0,28	0,24	0,16						
9	7,03	8,52	0,02	82,16	1,88	0,35	0,04													
10	60,54		0,01	37,47	0,68	1,30														
11 (504A)	98,63	1,18	0,01		0,18															
12 (504B)	67,88	1,85	0,01	29,82	0,29	0,11	0,02	0,01												
1M	5,76	12,29	0,02	76,79	4,32	0,79	0,03	0,01												
2M	98,63	0,29	0,01	1,00	0,06			0,01												
3M	98,56	0,40	0,01	0,47	0,13	0,43		0,01												
4M	44,14	3,20	0,01	51,53	0,98	0,13		0,01												
5M	87,52	1,76	0,01	9,96	0,50	0,08		0,01	0,10	0,05										
6M	39,31	1,88	0,02	58,18	0,38				0,24											
7M	48,86		0,02	51,02	0,10															
8M	5,58	0,42	88,91	1,45	0,08					0,25	2,15		1,13	0,03						
9M	60,14	0,84	0,01	38,35	0,36			0,01	0,29											
1P	80,98	5,20		9,74	0,73	0,08		0,01	1,52		1,57					0,15				

2P	93,00	0,40		1,87	0,10	0,05		0,01	2,02		2,34	0,19				0,01				
3P	94,12			1,65	0,04				1,56		2,57					0,06				
4P	93,25	2,94		3,09					0,61										0,11	
5P	90,57	1,19		3,24	0,26				2,16		2,57									
6P	91,38			1,64	0,07				2,33		4,36	0,18				0,05				
7P	77,45	2,39		17,21	0,41				0,98		1,23					0,23				0,10

Table 4. Peak position (cm^{-1}) and values of ratios of peak areas for the studied ochres.

	Peak position (cm^{-1})						Peak ratios			
Sample	a	b	c	d	e (double)		b/a	b/c	b/d	b/e
12 (EU 504)	226	296	412	499	612	661	1,87	2,12	5,39	2,41
2 (EU 17)	226	293	406	496	612	664	1,76	1,85	5,74	1,47
1M	226	293	409	496	612	659	1,59	1,72	3,95	0,84
2P	229	293	409	490	609	656	1,64	2,04	6,13	0,85

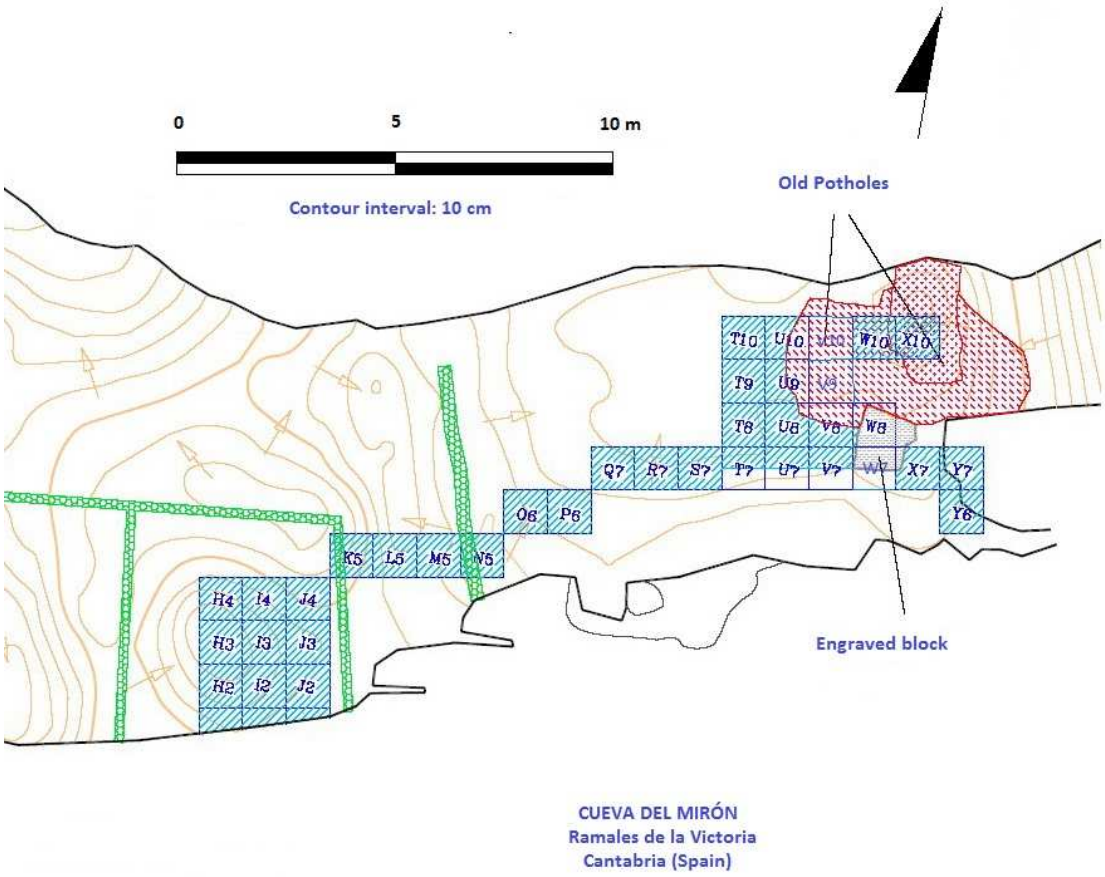

Figure 1. Plan of the El Mirón Cave vestibule showing the excavation areas (drawn by E. Torres).

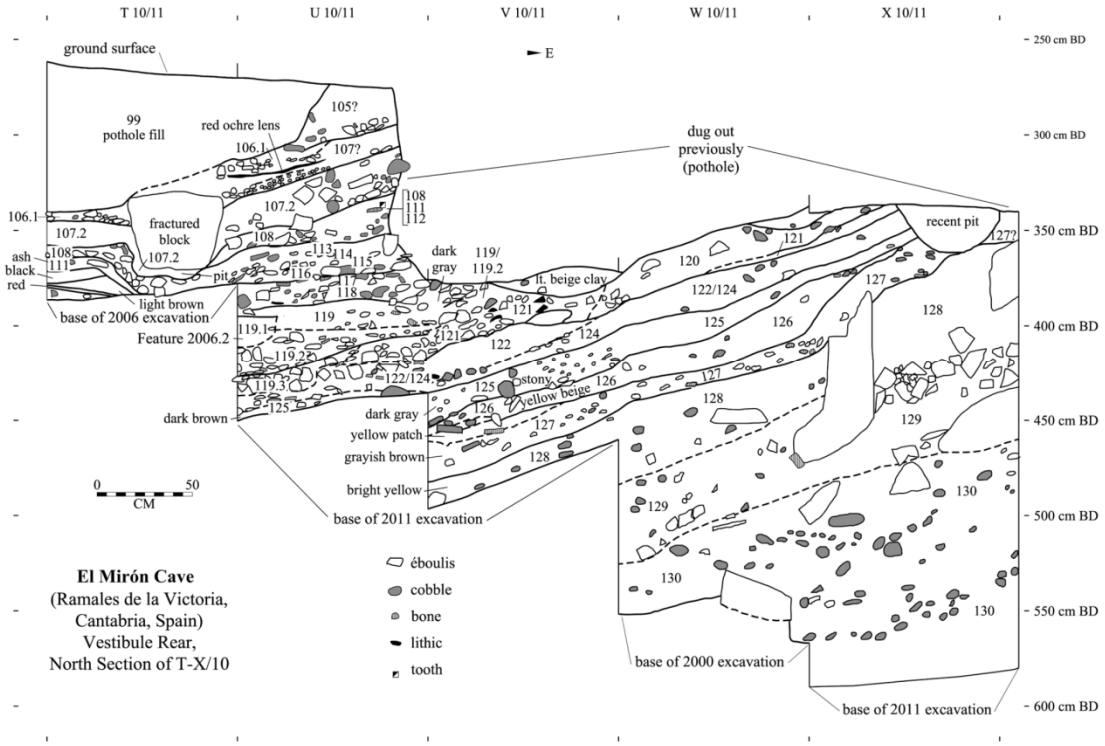

Figure 2. North stratigraphic section of squares T-X/10 (drawn by L.G. Straus, redrafted by R. Stauber).

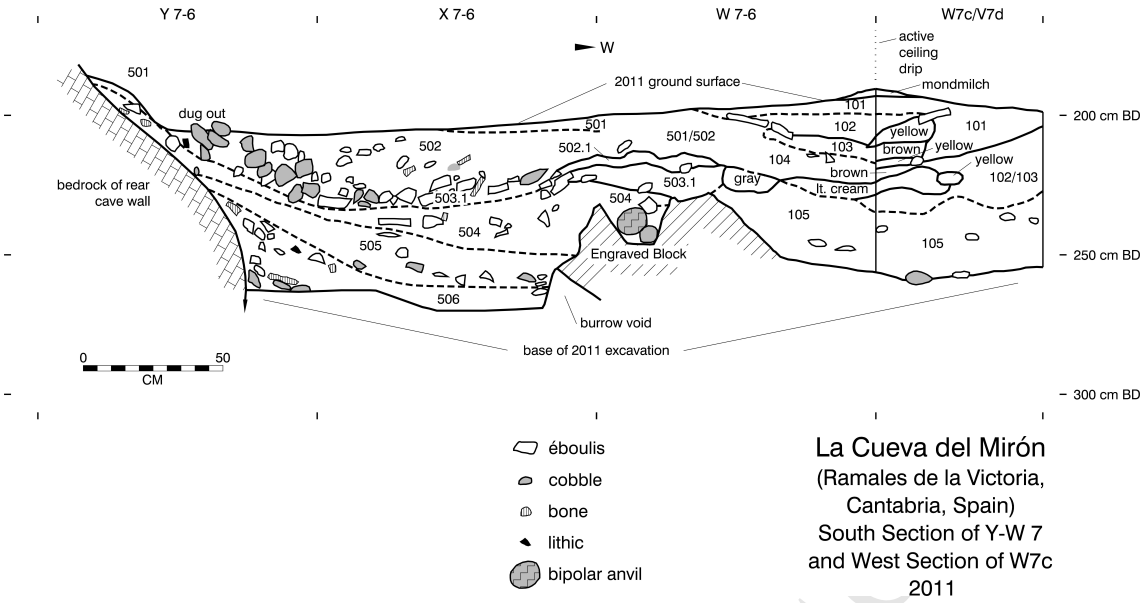

Figure 3. South stratigraphic section between X-Y7 and X-Y6 in the middle of the burial area, plus west section of W7c (W7c/V7d) connecting the burial area to the main Vestibule Rear excavation area (L.G. Straus and R. Stauber).

Figure 4. Photo of the south stratigraphic section between X-Y7 and X-Y6 (Romualdo Seva).

Figure 5. Compacted sediment showing the interface between the layers 503 and 504.

Figure 6. Initial and lower Magdalenian Ochres (1-9), and EU 504 (10-12).

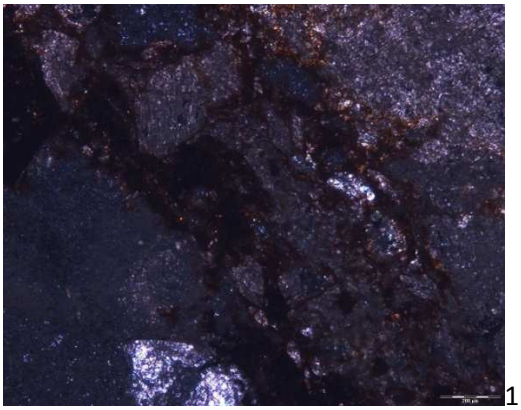
1

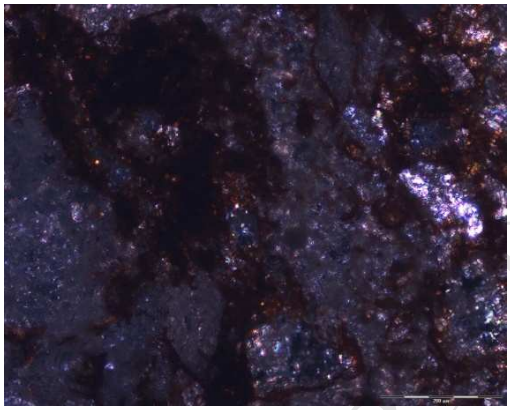
2

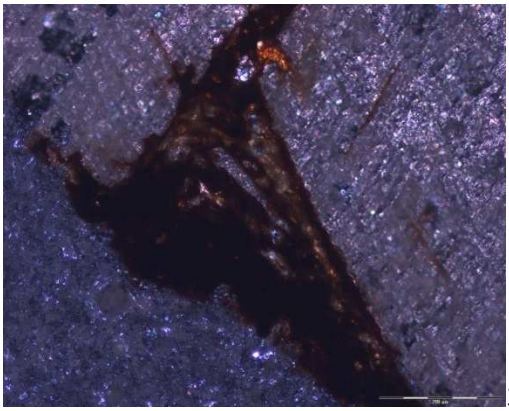
3

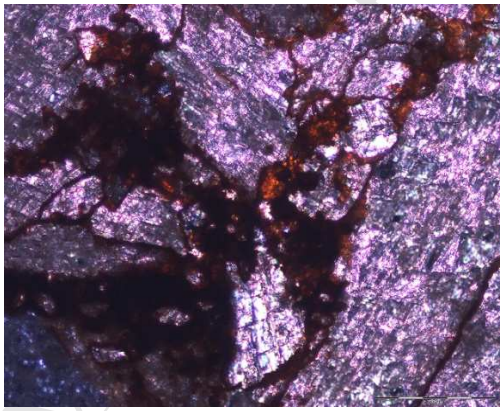
4

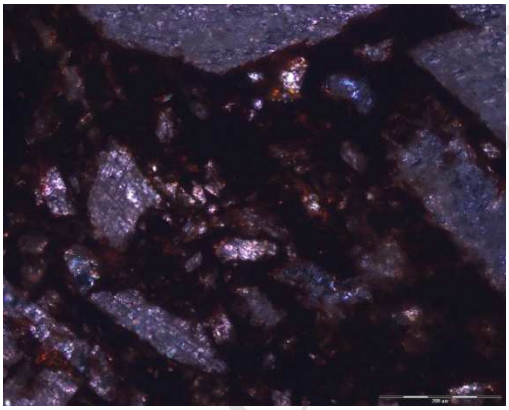
5

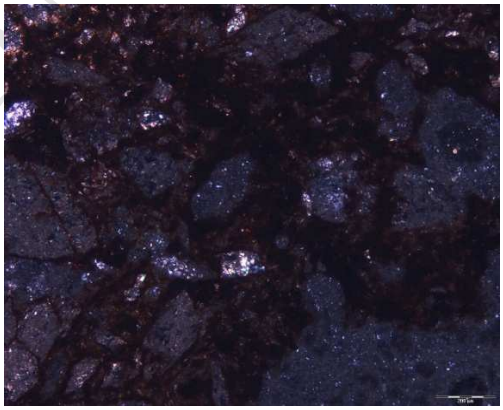
6

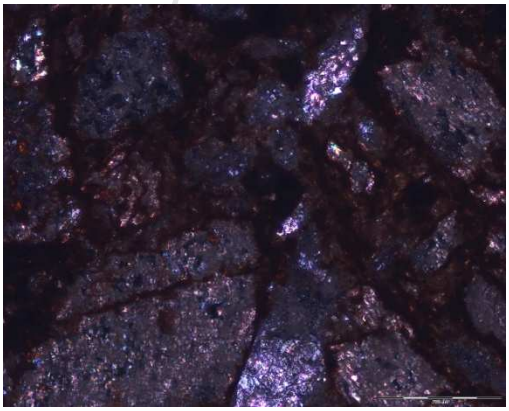
7

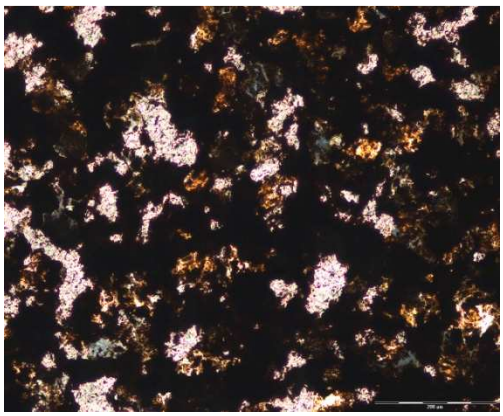
8

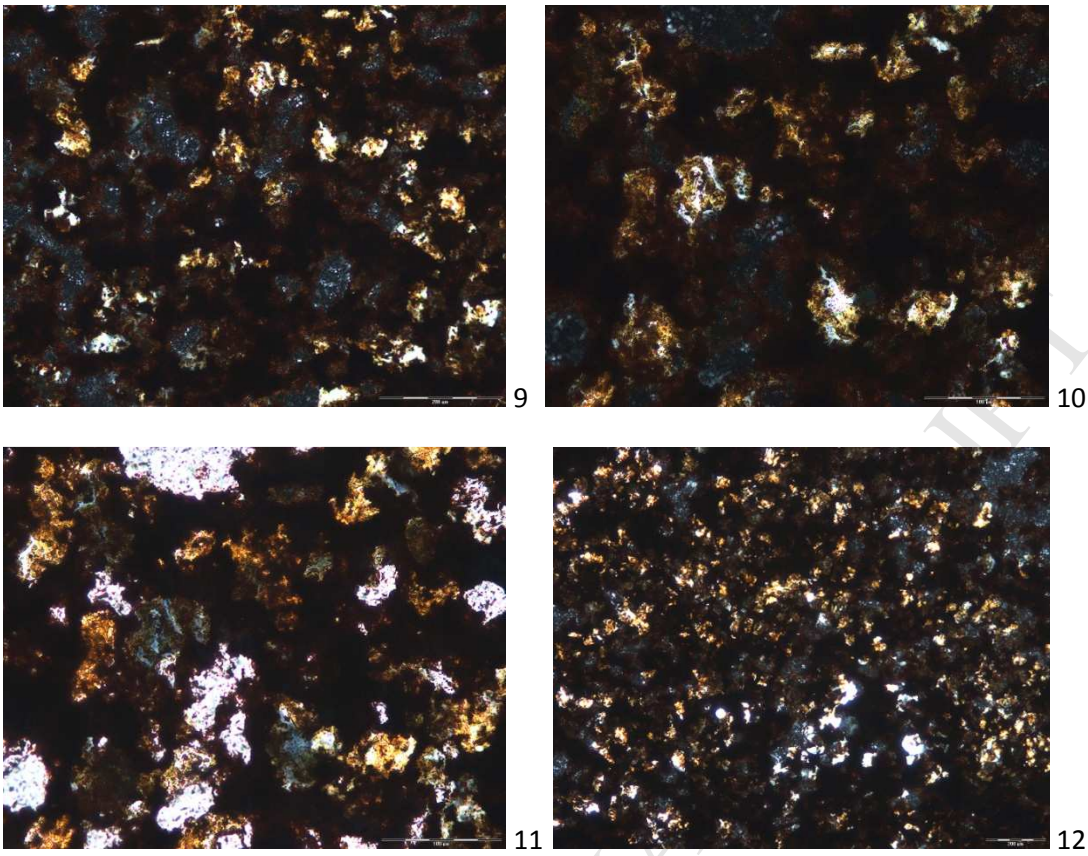

Figure 7. Images obtained by thin section of sample 3P (1-7) and ochre 504 level at different magnifications. x10 (8-9); x20 (10-11); x5 (12). .

a)

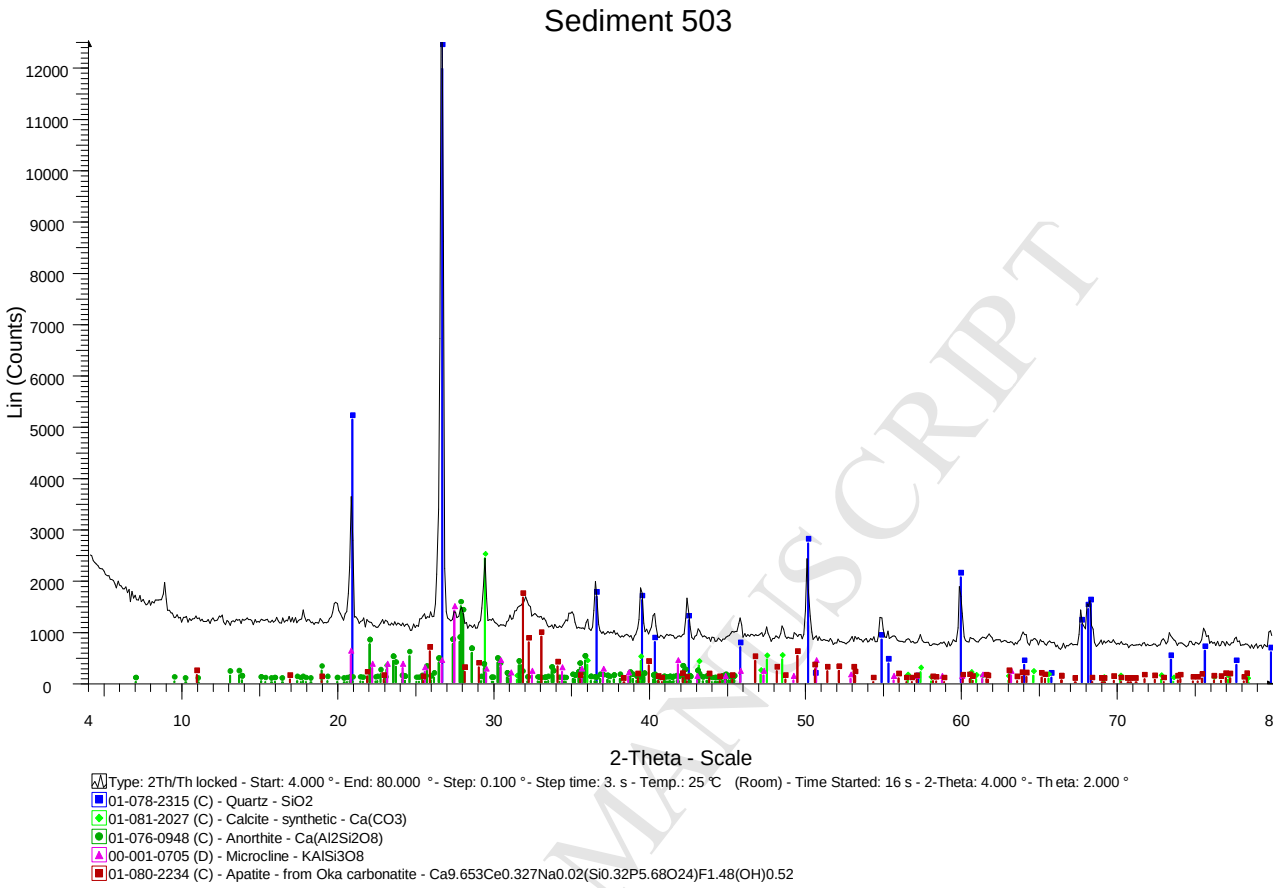

b)

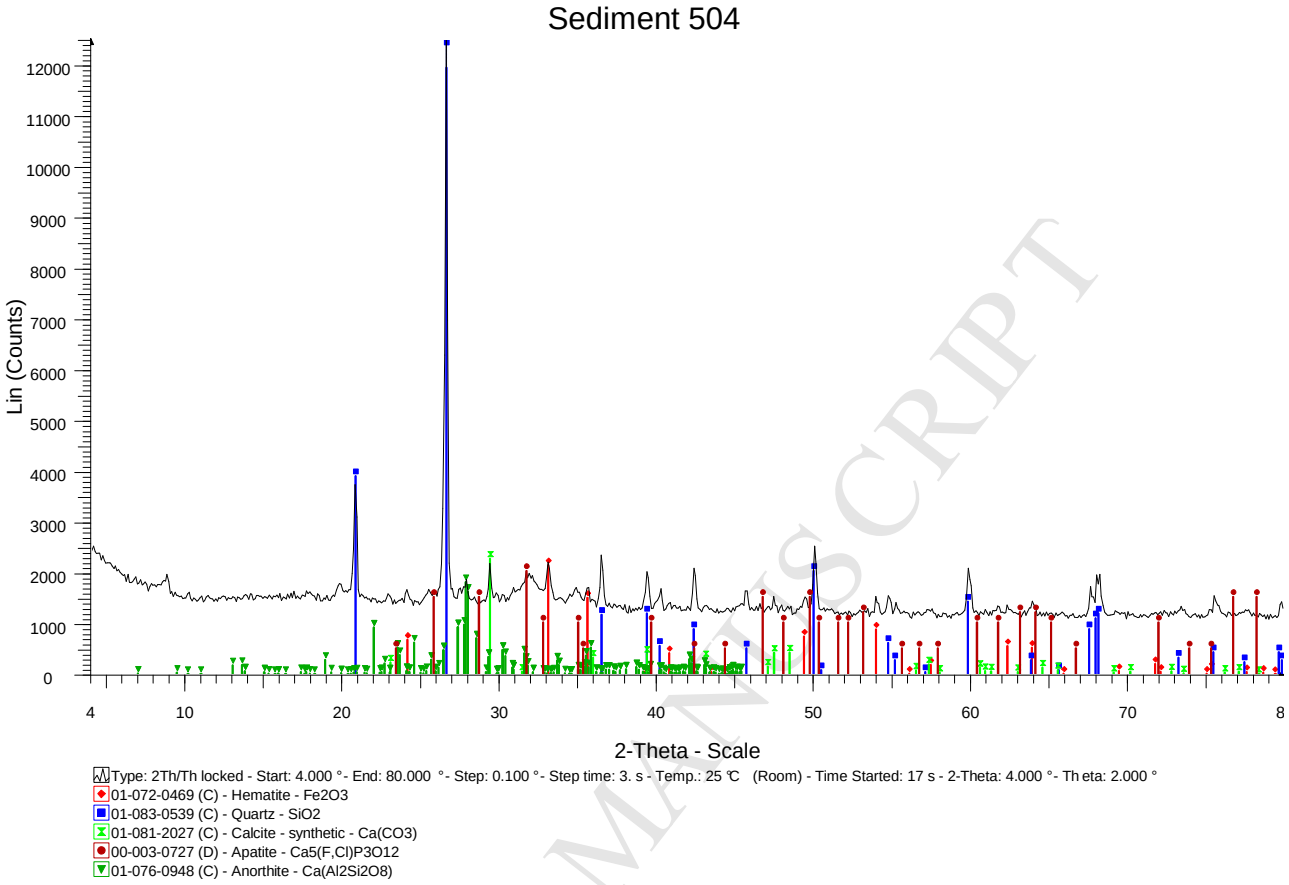

c)

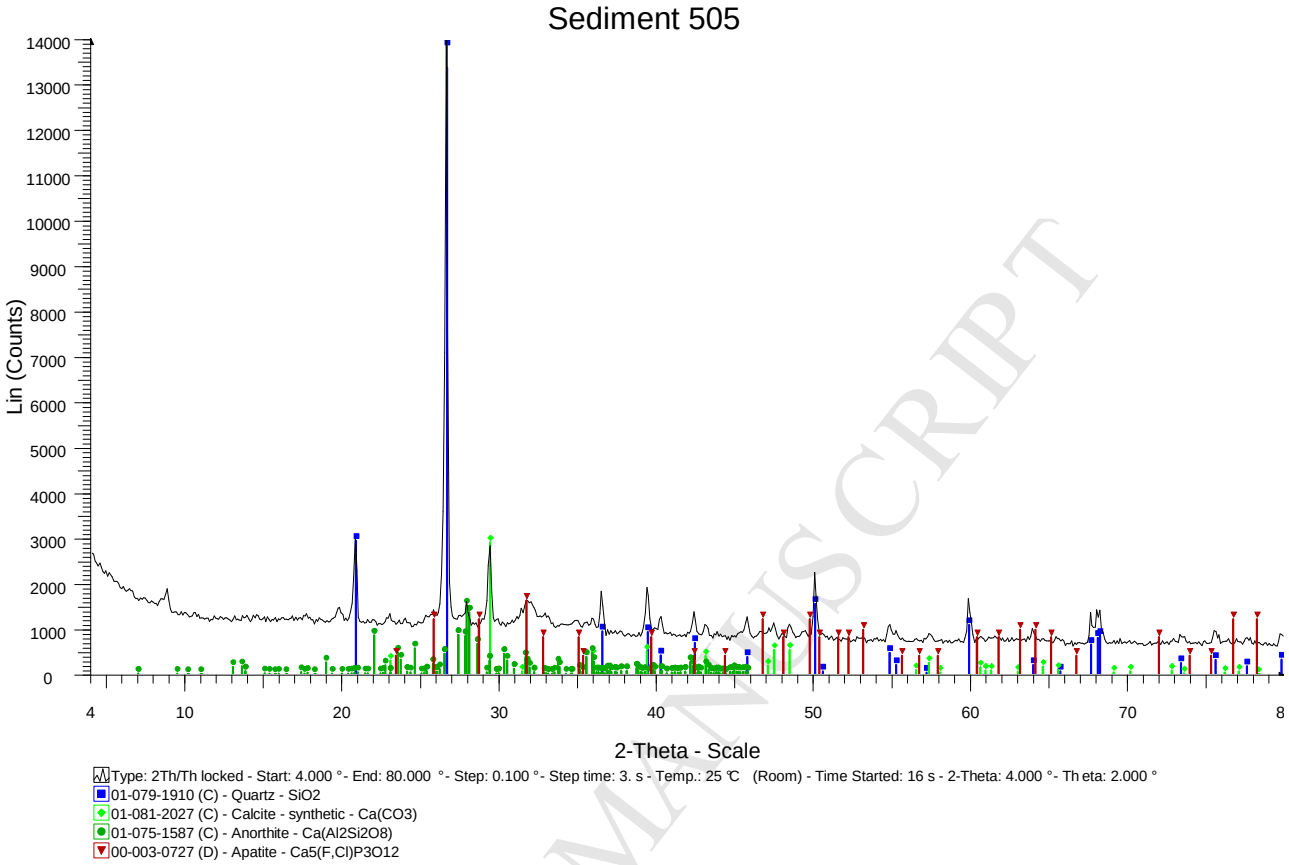

d)

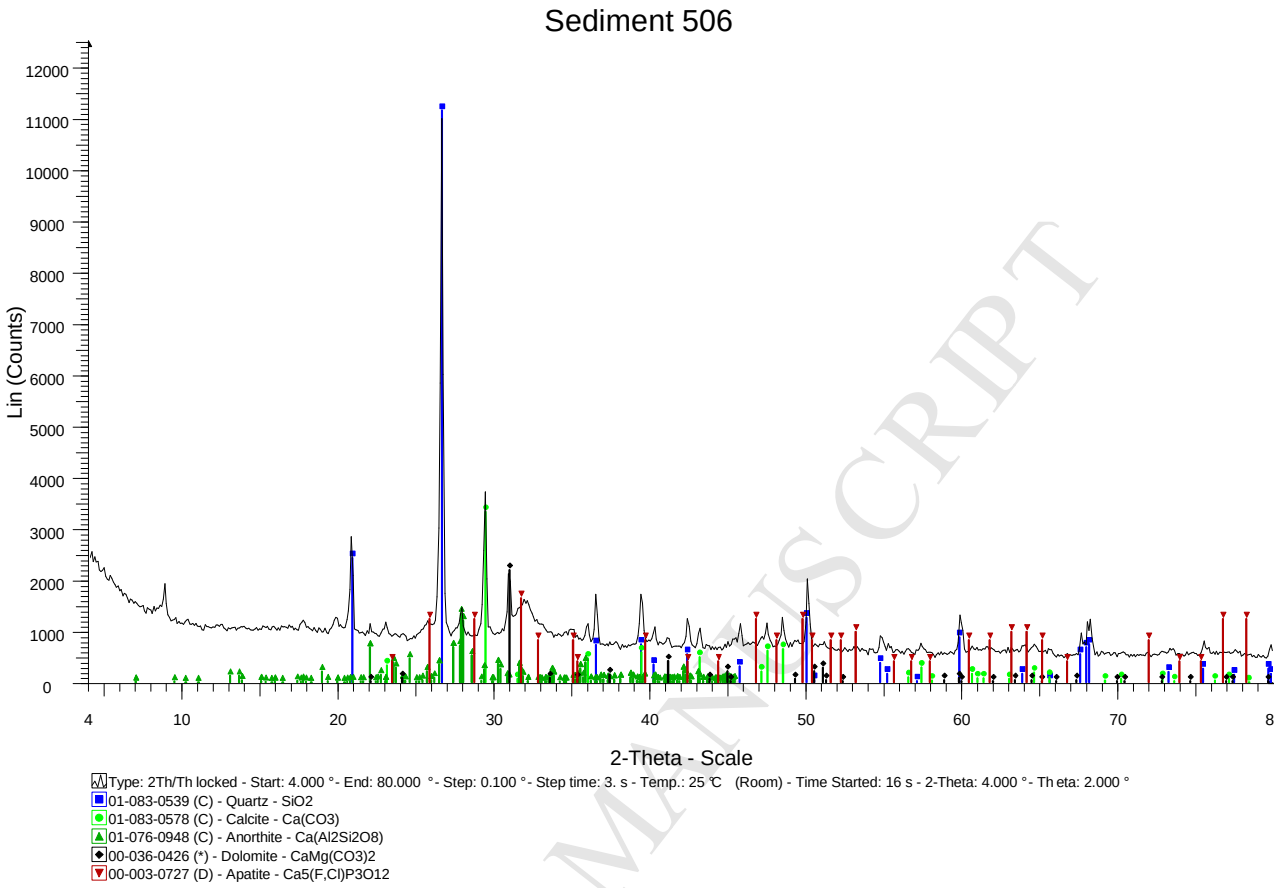

e)

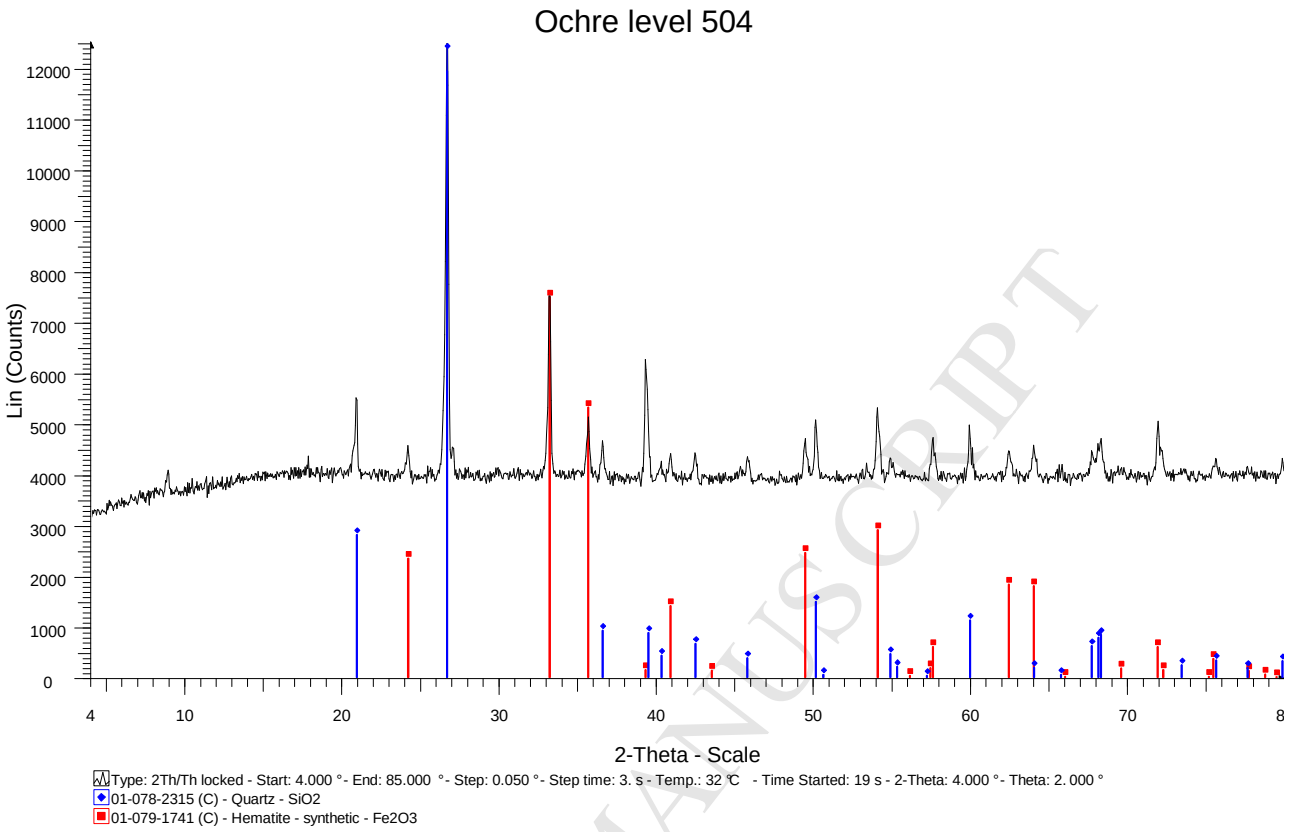

Figure 8. Diffractograms of layers 503-506 (a-d) and crystalline fragment (hematite) of layer 504 (e).

a) Level 504 ochre (fragment 1).

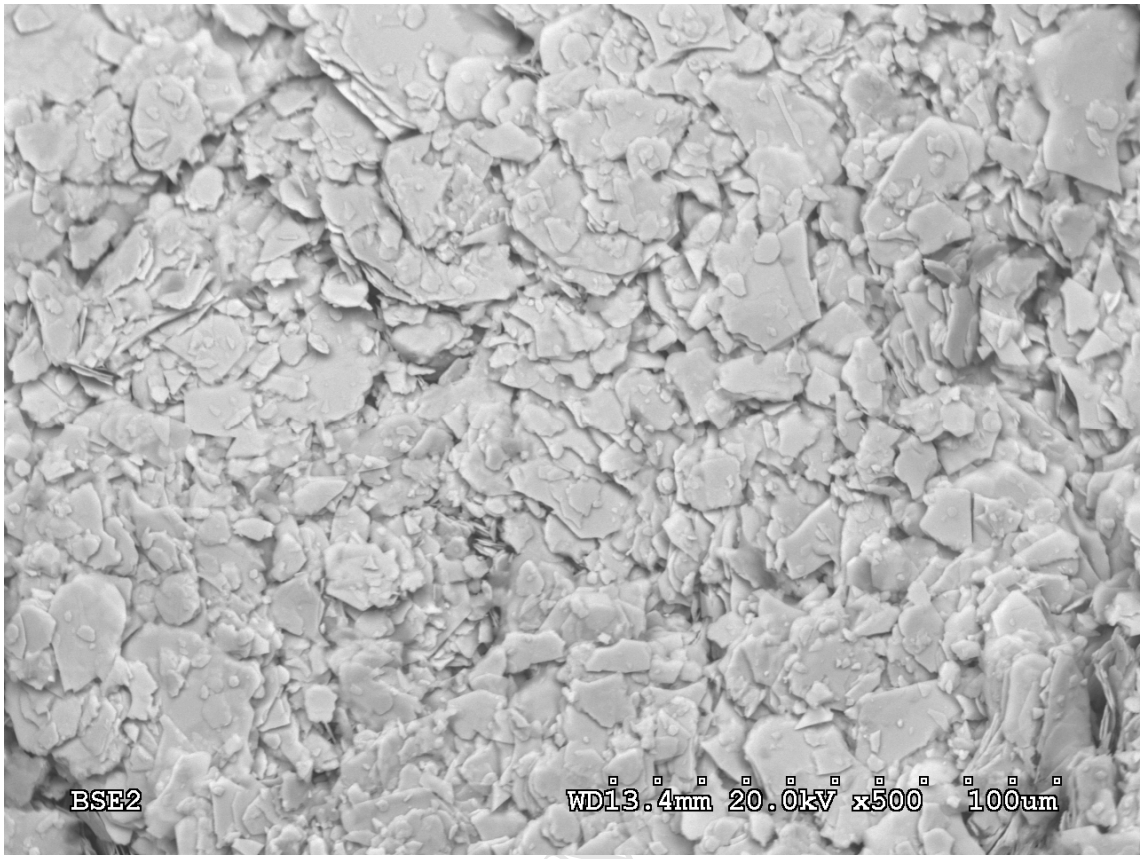

b) Level 504 ochre (fragment 2).

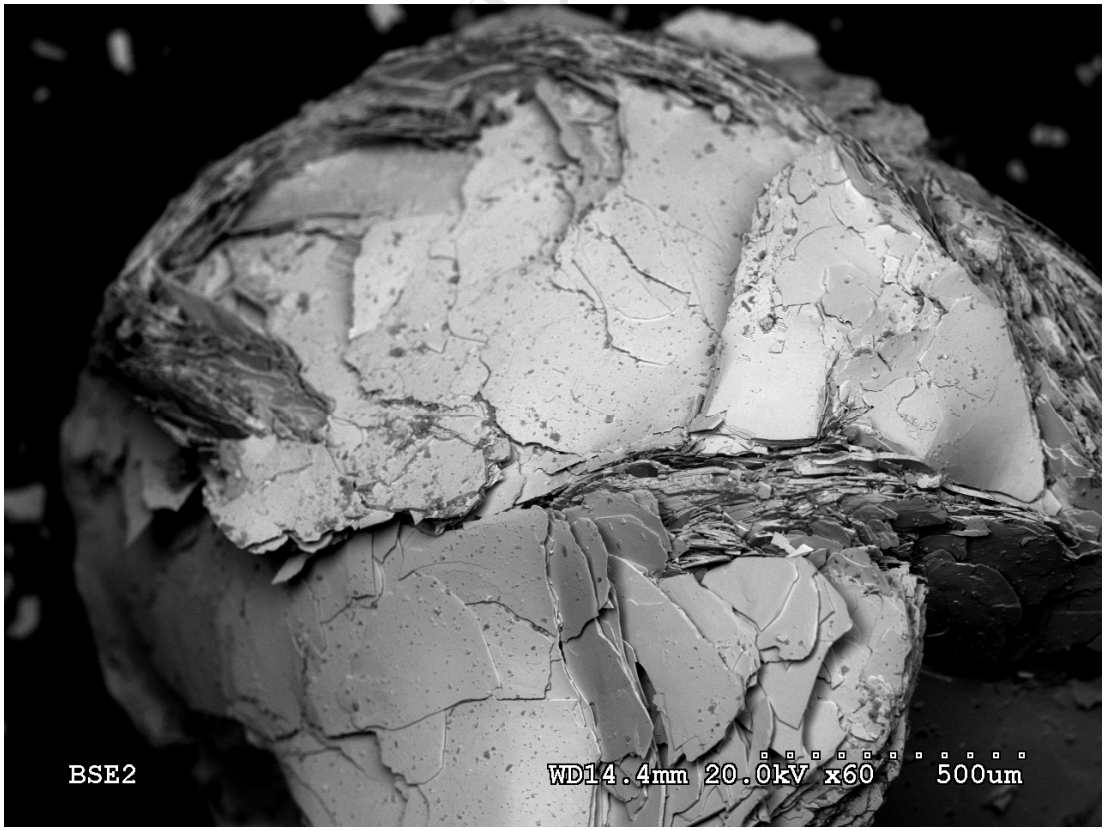

c) Level 504 ochre (fragment 3).

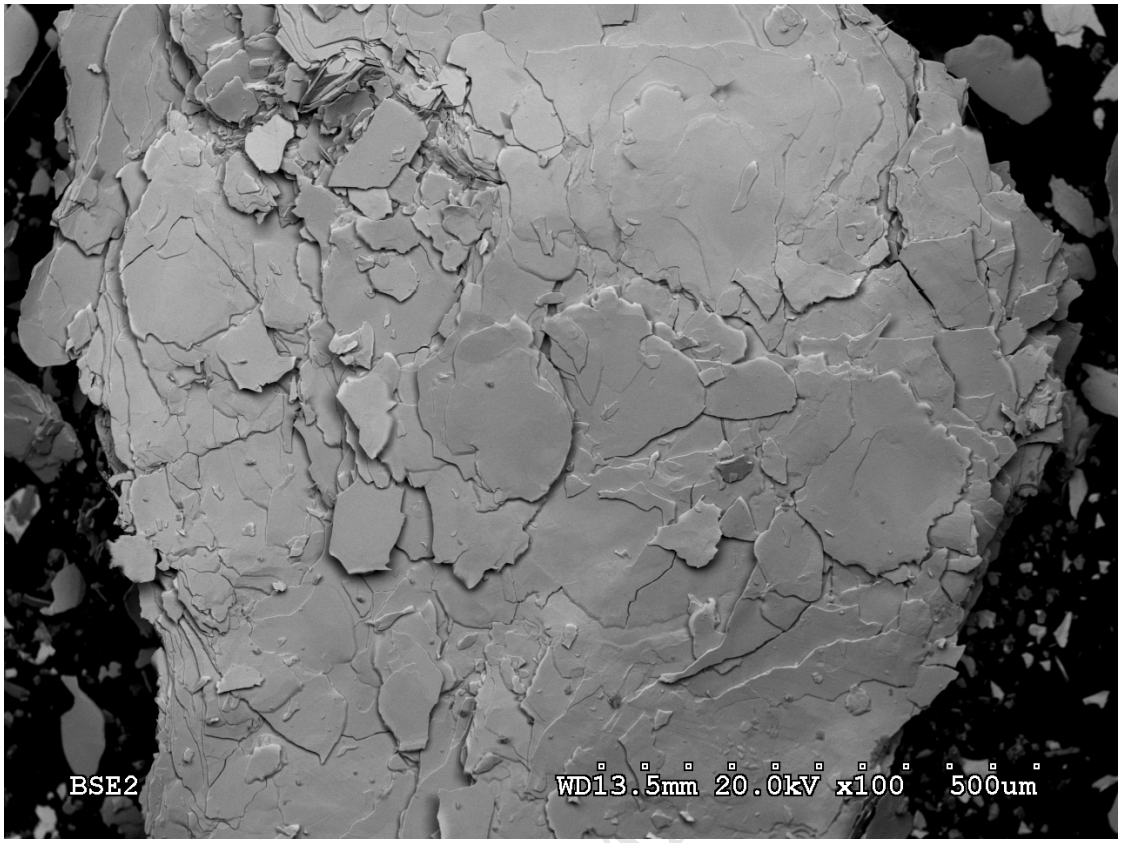

d) Sediment with ochre (level 504).

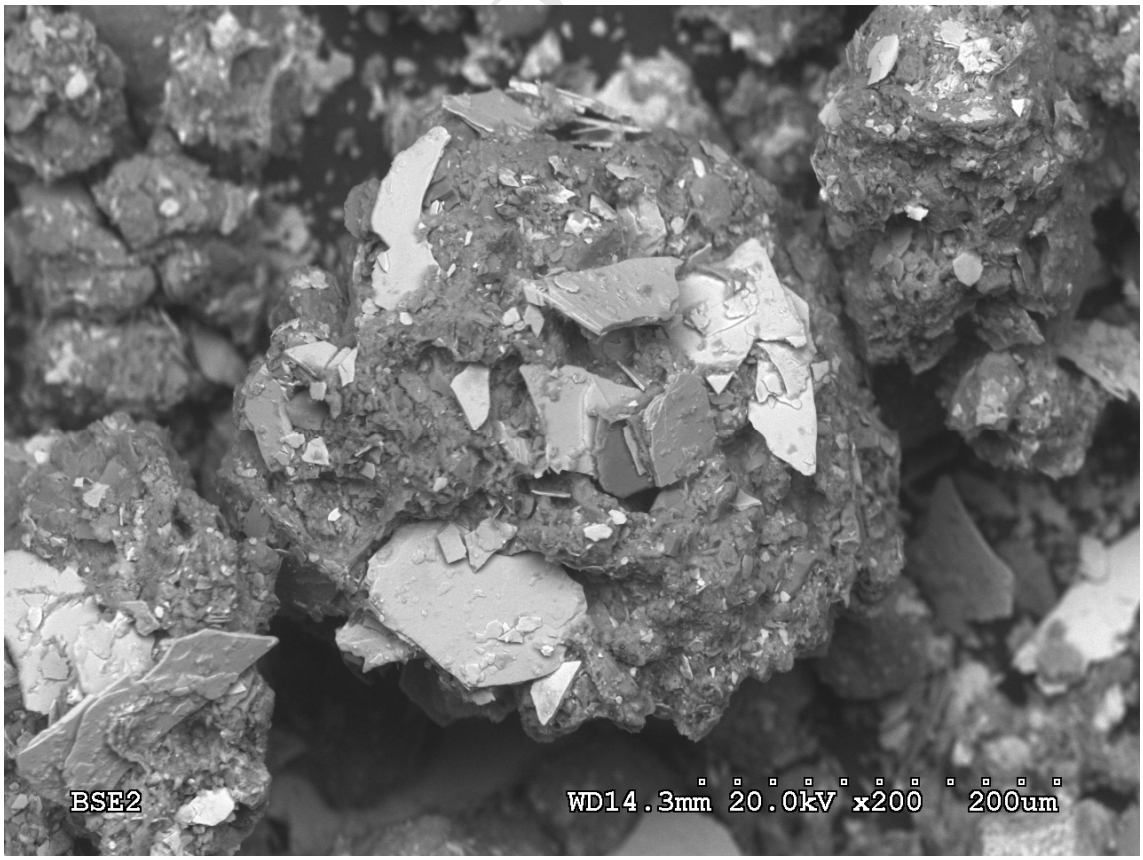

e) Carranza Valley, prospected sample (2P)

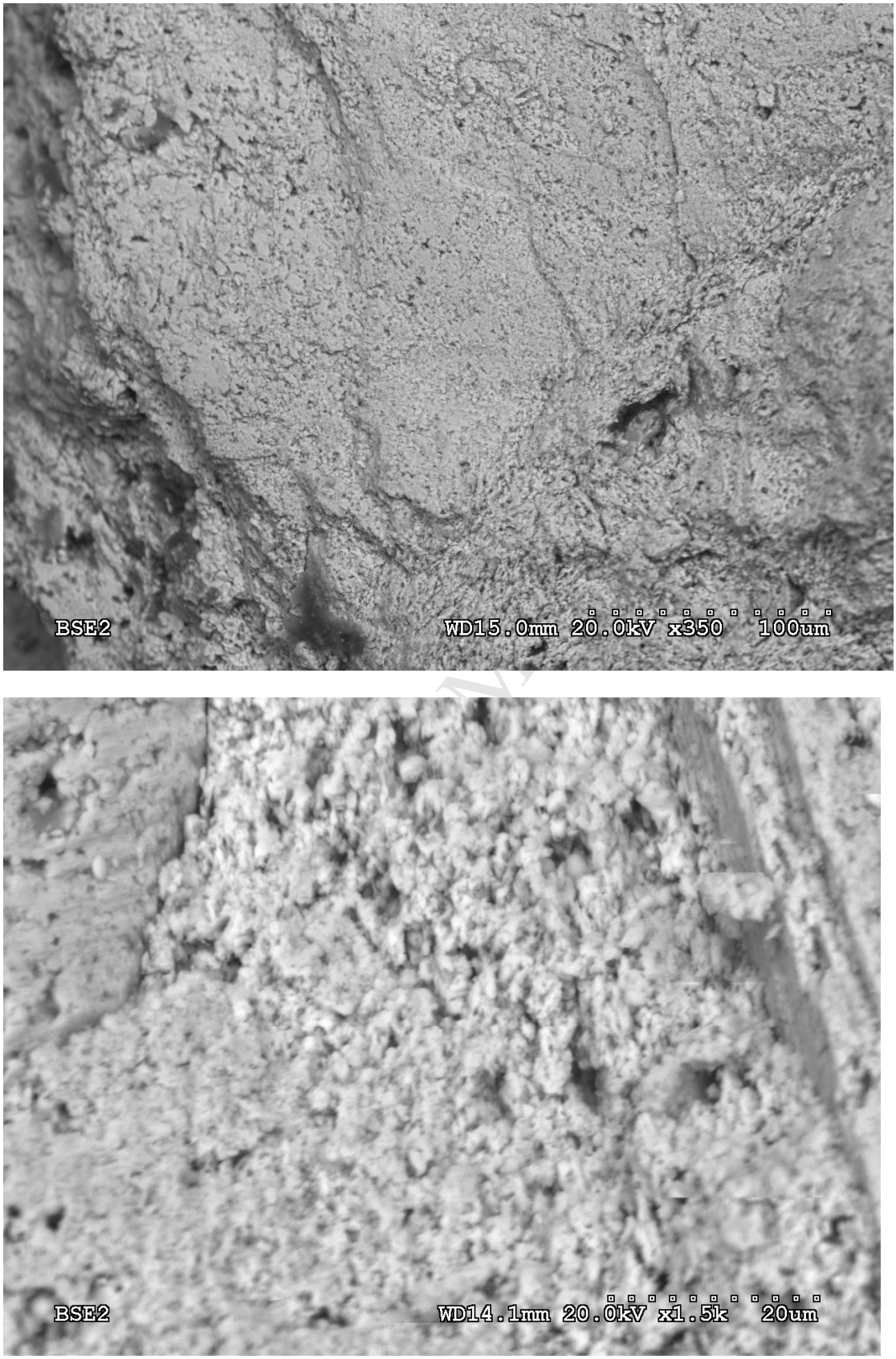

Figure 9. SEM images of ochre and sediment samples.

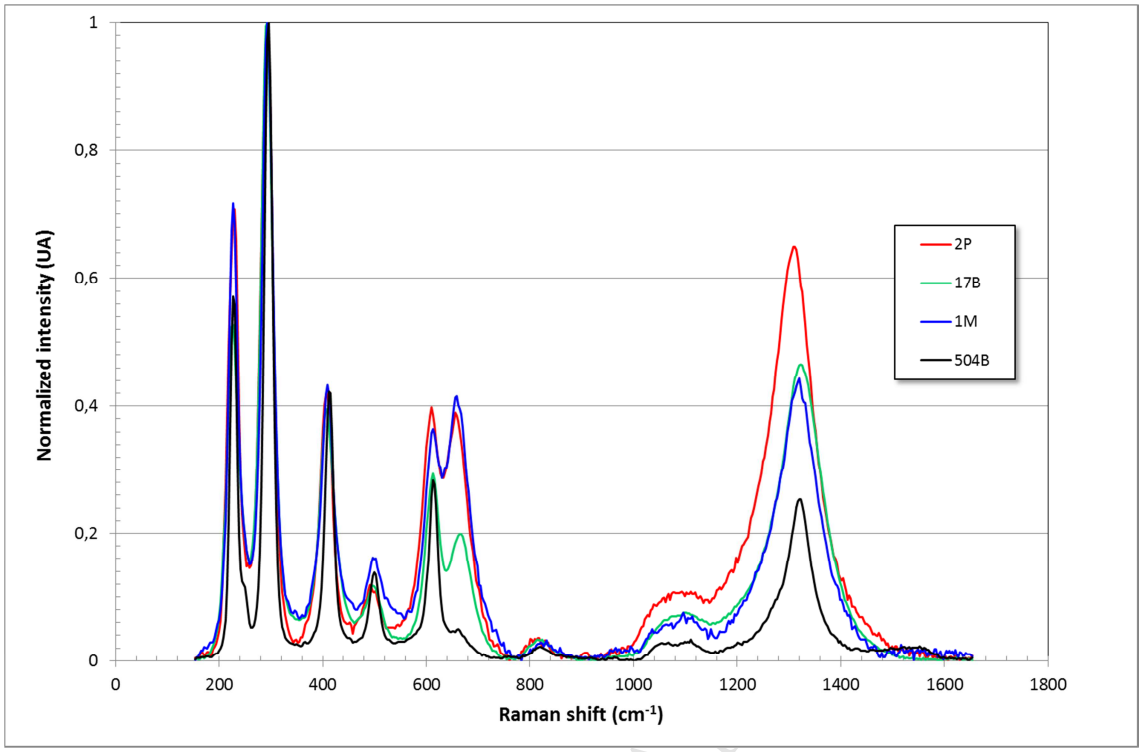

Figure 10. Raman spectra of samples of different levels of El Mirón (17B, 504B and 1M) and a sample of the prospection (2P).

```
FACTOR
  /VARIABLES Th U Li Mo Cr Co V Ni Cu Zn Ga Se Cd In Tl Bi Be Sr Cs Sn
  /MISSING MEANSUB
  /ANALYSIS Th U Li Mo Cr Co V Ni Cu Zn Ga Se Cd In Tl Bi Be Sr Cs Sn
  /SELECT=Au(0)
  /PRINT UNIVARIATE INITIAL CORRELATION DET KMO INV AIC EXTRACTION ROTATION
  /CRITERIA FACTORS(3) ITERATE(25)
  /EXTRACTION PC
  /CRITERIA ITERATE(25)
  /ROTATION VARIMAX
  /SAVE REG(ALL)
  /METHOD=CORRELATION.
```

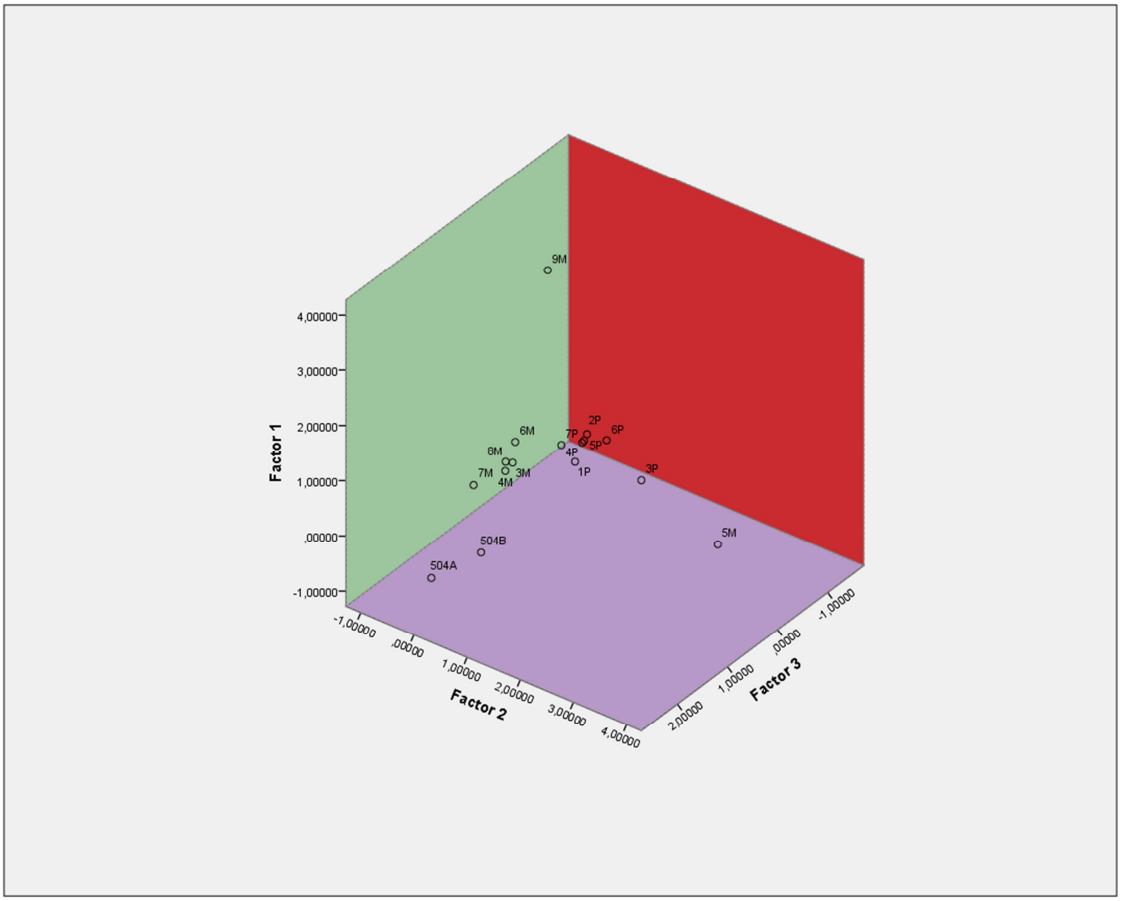

Figure 11. Principal Component Analysis applied to the data obtained by ICP-MS.

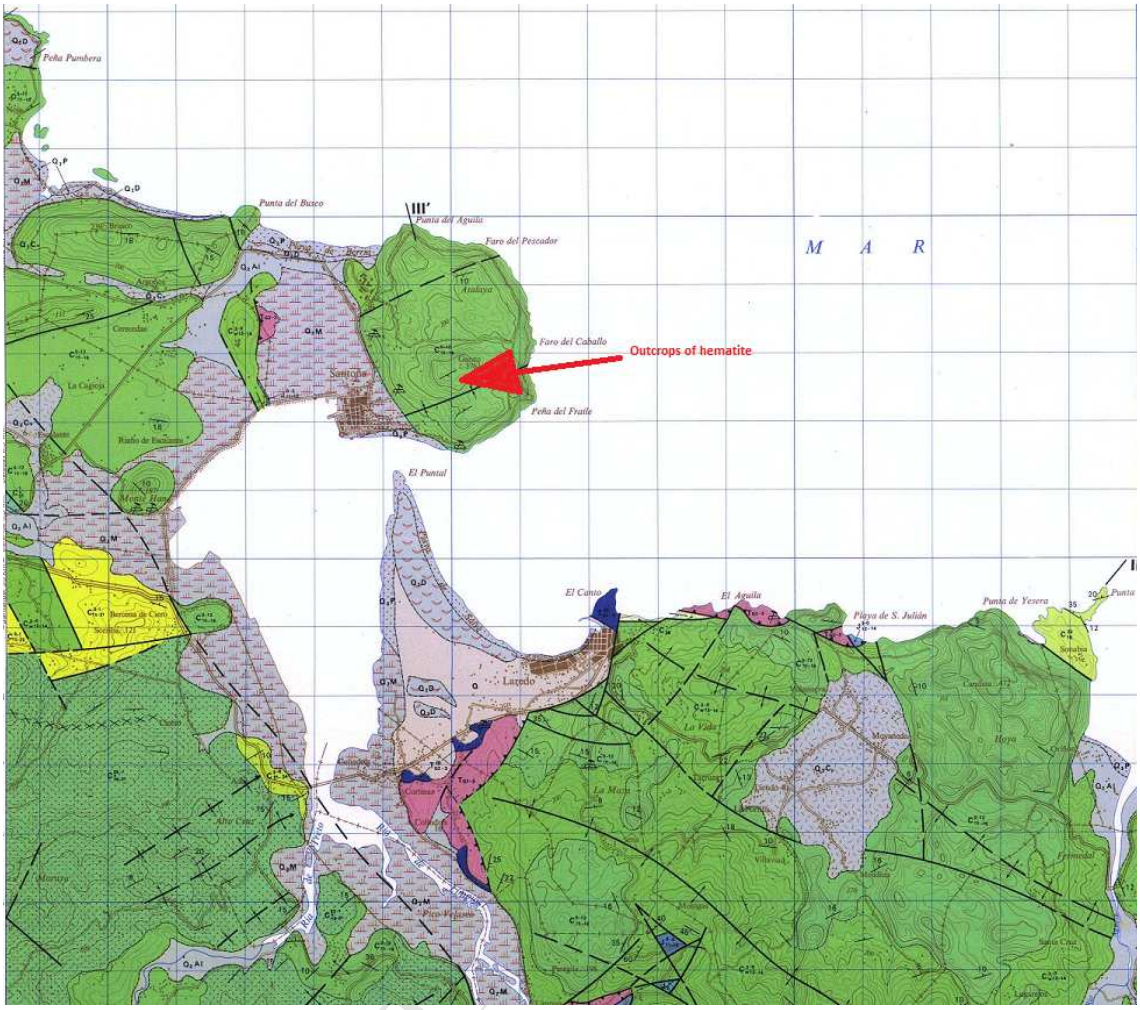

Geological map of outcrops of hematite in Santoña. (IGME-Sheet nº36). Key: C_{15-16}^{0-12}, limestone with rudists and orbitolins.